

Formation of mass gap compact object and black hole binary from Population III stars

Tomoya Kinugawa¹, Takashi Nakamura², and Hiroyuki Nakano³

¹*Institute for Cosmic Ray Research, The University of Tokyo, Kashiwa, Chiba 277-8582, Japan*

²*Department of Physics, Graduate School of Science, Kyoto University, Kyoto 606-8502, Japan*

³*Faculty of Law, Ryukoku University, Kyoto 612-8577, Japan*

1/11/2021

.....
We performed population synthesis simulations of Population III binary stars with Maxwellian kick velocity distribution when MGCOs (Mass Gap Compact Objects with mass $2\text{--}5 M_{\odot}$) are formed. We found that for eight kick velocity dispersion models of $\sigma_k = 0\text{--}500$ km/s, the mean mass of black hole (BH)-MGCO binary is $\sim (30 M_{\odot}, 2.6 M_{\odot})$. In numerical data of our simulations, we found the existence of BH-MGCO binary with mass $(22.9 M_{\odot}, 2.5 M_{\odot})$ which looks like GW190814.
.....

Subject Index xxxx, xxx

1. *Introduction* GW190814 [1] is a gravitational wave (GW) event observed by LIGO-Virgo collaboration during the first half of the third observation period, called O3a. This is a compact binary coalescence and the parameter estimation suggests that the binary consists of a black hole (BH) with mass of $22.2\text{--}24.3 M_{\odot}$ and a compact object with mass of $2.50\text{--}2.67 M_{\odot}$ yielding a chirp mass of $M_{\text{chirp}} \sim 6.03\text{--}6.15 M_{\odot}$ ¹. The mass of the smaller (secondary) object lies in $2\text{--}5 M_{\odot}$, that is, between known neutron stars (NSs) and BHs. Therefore, the secondary compact object will be a NS with the maximum observed mass or a BH with the minimum observed mass, so that we define a mass gap compact object (MGCO)² as a compact object having mass $2\text{--}5 M_{\odot}$. The merger rate density of this type of binaries is estimated as $1\text{--}23 \text{ Gpc}^{-3} \text{ yr}^{-1}$ [1]. So far, many proposals and discussions on the BH-MGCO binary with MGCO mass of $\sim 2.6 M_{\odot}$ were appeared after the announcement of GW190814 (see, e.g., Refs. [3–24]).

We discussed in our previous study [25] in 2016, the detection rate and the chirp mass distribution of NS-BH binaries with mass of NS below $3 M_{\odot}$ by the population synthesis simulations of Population III (Pop III) stars. We found that the merger rate density of Pop

¹ $M_{\text{chirp}} = (m_1 m_2)^{3/5} / (m_1 + m_2)^{1/5}$ where m_1 and m_2 denote the mass of the primary and the secondary objects, respectively.

² MGCO is different from “mass gap” ($2.5\text{--}5 M_{\odot}$) used in Ref. [1] and “MassGap” ($3\text{--}5 M_{\odot}$) defined in Ref. [2]. MGCOs include not only MassGap BHs, but also NSs with mass $\gtrsim 2 M_{\odot}$, i.e., the mass of MGCOs lies in $2\text{--}5 M_{\odot}$.

III NS-BH binaries is $\sim 1 \text{ Gpc}^{-3} \text{ yr}^{-1}$ although it depends on the natal kick velocity of NSs. We also found that the chirp mass distribution of Pop III NS-BH binaries that merge within the Hubble time has a peak around $6 M_{\odot}$.

The results presented in Ref. [25] seems to be consistent with the estimation of Ref. [1] since in Ref. [25] we defined NS if its mass is below $3 M_{\odot}$ while the mass of secondary of GW190814 is $2.50\text{--}2.67 M_{\odot}$ and the chirp mass of GW190814 is evaluated as $6.03\text{--}6.15 M_{\odot}$. Thus, it is important to revisit our previous paper using the definition of MGCO and try to answer the question raised as follows. What are “the processes by which the lightest BHs or the most massive NSs form” in Ref. [1] ?

In this letter, we summarize our previous study with additional analyses, and present a scenario to explain the BH-MGCO binary of GW190814.

2. *Analysis* In Ref. [25], we have calculated NS-BH formations and estimated the number of NS-BH binaries merging within the Hubble time by using the population synthesis simulations of Pop III stars [26]. The key ingredient is to introduce the NS kick velocity of $200\text{--}500 \text{ km/s}$ that is evaluated from the observation of the proper motion of the pulsar. The effect of kick velocity is important to decrease the merging time of NS-BH binaries. For comparison, we have calculated not only the Pop III NS-BH binaries, but also Pop I and II NS-BH binaries.

To do the above analysis in our population synthesis Monte Carlo simulations, we have considered six metallicity cases from $Z = 0$ (Pop III) to $Z = Z_{\odot}$ (Pop I) where Z_{\odot} is the solar metallicity, the initial mass, mass ratio, separation and eccentricity distribution functions as binary initial conditions, the Roche lobe overflow, the common envelope phase, the tidal effect, the supernova (SN) effect, and the gravitational radiation as binary interactions, and two kick velocity models with $\sigma_k = 265 \text{ km/s}$ and $\sigma_k = 500 \text{ km/s}$ where σ_k is the dispersion of a Maxwellian distribution for kick velocity.

Next, we briefly summarize the results. The chirp mass of Pop III NS-BH binaries merging within the Hubble time is heavier than those of Pop I and II ones. The peak values of chirp mass distributions is $\sim 6 M_{\odot}$ in the case of Pop III while it is $\sim 2 M_{\odot}$ in the cases of Pop I and II. These peak values almost do not depend on the kick velocity values σ_k .

The NS-BH merger rates at the present day depend on the progenitors and kick velocities (see Table 3 in Ref. [25] for the details). The sum of the merger rates of Pop I and II becomes $19.7 \text{ Gpc}^{-3} \text{ yr}^{-1}$ and $6.38 \text{ Gpc}^{-3} \text{ yr}^{-1}$ for $\sigma_k = 265 \text{ km/s}$ and 500 km/s , respectively. For the Pop III case, we have found the NS-BH merger rates at the present day as $1.25 \text{ Gpc}^{-3} \text{ yr}^{-1}$ and $0.956 \text{ Gpc}^{-3} \text{ yr}^{-1}$ for $\sigma_k = 265 \text{ km/s}$ and 500 km/s , respectively. In the previous study, we have assumed that the mass range of neutron stars are $1.44\text{--}3 M_{\odot}$. Thus, GW190814 belongs to the previous Pop III NS-BH result.

In this letter, we further focus on compact object binaries which consist of a BH and a MGCO with mass of $2\text{--}5 M_{\odot}$. We calculate 10^6 Pop III binary evolutions and the merger rates of BH-MGCO binaries, using the same setup of the previous Pop III NS-BH case [25]. For simplicity, we use the simple SN remnant model given in Refs. [26, 27] which is consistent with the red supergiant problem within error [28]. A low mass progenitor whose CO core mass is small ($M_{\text{CO}} \lesssim 5 M_{\odot}$) experiences a SN and the Fe core remains as the remnant. On the other hand, a high mass progenitor ($M_{\text{CO}} \gtrsim 7.6 M_{\odot}$) becomes a direct collapse, and the whole stellar mass becomes the remnant mass. An intermediate progenitor ($5 M_{\odot} \lesssim M_{\text{CO}} \lesssim$

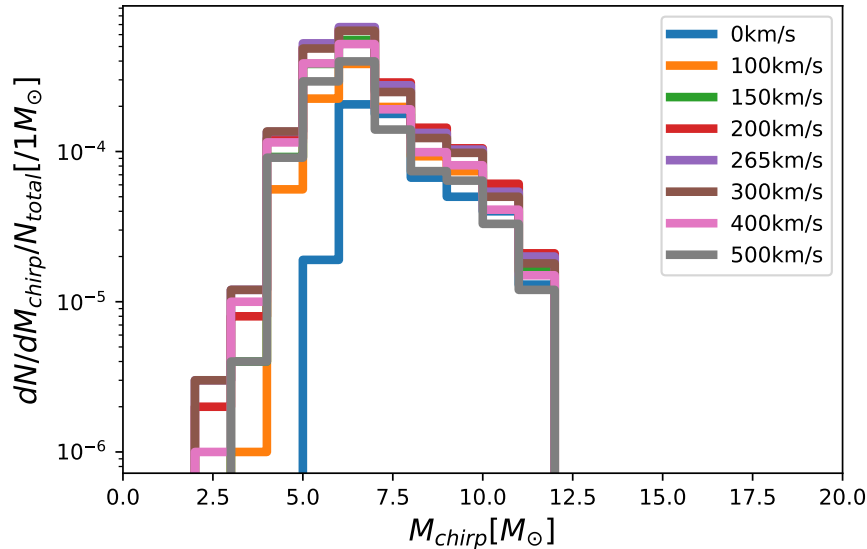


Fig. 1 The chirp mass distribution of BH-MGCO binaries which merge within the Hubble time for 8 kick models with $\sigma_k = 0, 100, 150, 200, 265, 300, 400,$ and 500 km/s, where $N_{\text{total}} = 10^6$ is the total number of binaries which we have simulated. The chirp mass distribution does not strongly depend on the kick velocity. The averaged individual masses are summarized in Table 1.

$7.6 M_{\odot}$) experiences a failed SN and the fall backed remnant mass linearly increases with increasing progenitor mass.

Here, we assume that the SN remnants which have a mass less than $5 M_{\odot}$ experience SN kick, and we use the Maxwellian distribution for the kick velocity distribution. We calculate not only kick velocity dispersion models of the previous paper of $\sigma_k = 265$ km/s and 500 km/s, but also $\sigma_k = 100, 150, 200, 300,$ and 400 km/s.

Results are shown by Figs. 1 and 2. Figure 1 shows the chirp mass distribution of BH-MGCO binaries which merge within the Hubble time for each model, where $N_{\text{total}} = 10^6$ is the total number of binaries which we have simulated. The chirp mass distribution does not strongly depend on the kick velocity and has a peak at $M_{\text{chirp}} \sim 6 M_{\odot}$. Notice here that the chirp mass of GW190814 is $\sim 6 M_{\odot}$. Figure 2 shows the merger rate densities for each model. The peak of merger rate density depends on the kick velocity. Almost all BH-MGCO binaries cannot merge within the Hubble time without the natal kick. The natal kick changes the binary orbit and makes the binary be able to merge within the Hubble time. If the kick velocity is smaller than the orbital velocity of the BH-MGCO progenitor (\sim a few hundred km/s), the kick only affects as a perturbation like 100 km/s model, and the merger time of BH-MGCO tends to be still long (i.e., they merge at low redshift). However, if the kick velocity becomes more than the orbital velocity of the BH+MGCO progenitor, the orbit of BH-MGCO can be determined by the kick. In this case, the kick sometimes brakes the orbit and the orbit of BH-MGCOs becomes so close that they can merge with a short merger time. Thus, the peak of merger rate density asymptotically moves to near the peak of Pop III SFR

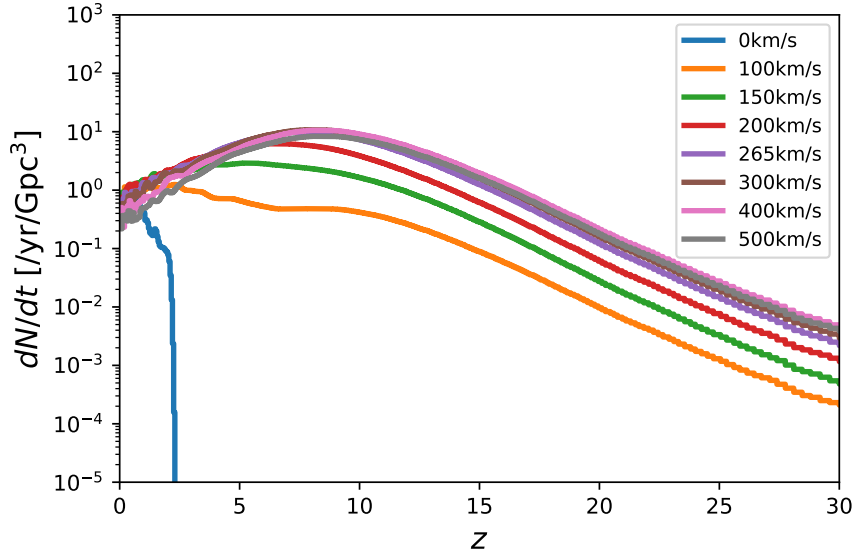


Fig. 2 The merger rate densities for 7 kick models with $\sigma_k = 100, 150, 200, 265, 300, 400,$ and 500 km/s. We note that the smaller kick velocity model, the lower redshift the peak of merger rate is.

($z \sim 10$). Furthermore, the number of BH+MGCO binaries decreases with the increasing σ_k . The merger rate slightly decreases at almost all red shift values if the kick is $\gtrsim 300$ km/s.

Since the typical chirp mass of BH-MGCO binary of $\sim 6M_\odot$ is almost the same as that of GW190814, we searched if similar BH-MGCO binary to GW190814 exists in our simulation data. As a result, we found one with mass $(22.9M_\odot, 2.5M_\odot)$. Figure 3 shows the evolutionary path of this binary. The binary is born as the zero age main sequence binary consisting of $54.7M_\odot$ and $14.3M_\odot$ stars. The primary evolves to a giant and starts a mass transfer. Next, the primary becomes so large that the secondary plunges into the primary envelope so that the binary enters common envelope phase. In the common envelope phase, the primary envelope is evaporated and the separation shrinks. Without natal kick, the mass ejection at the SN of secondary makes the binary too wide to merge within the Hubble time. However, if the direction of the natal kick is inverse to the orbital velocity, the binary is able to merge within the Hubble time. Figure. 3 shows that the final destiny of this binary is $22.9M_\odot$ BH and $2.5M_\odot$ compact object which is either the lightest BH or the most massive NS. This example might be a possible answer to the question of ‘‘What are the processes by which the lightest BHs or the most massive NSs form in Ref. [1] ?’’ in *Introduction*.

To estimate the event rate of Pop III BH-MGCO binaries, we use an inspiral-merger-ringdown waveform presented in Ref. [29] which is based on Refs. [30, 31], The signal-to-noise ratio (SNR) of GW events is calculated in 4 strain-noise fitted curves (see Fig. 4) which are prepared by using Ref. [32] for LIGO O3a-Livingston (O3a-L) (green) and LIGO O5 (magenta), Ref. [33] (see also Ref. [34]) for Einstein Telescope (ET-B) (red), and Ref. [35] for Cosmic Explorer (CE2) (purple). Then, for example, the maximum observable redshift z_{\max} by setting the averaged SNR = 8 for the GW190814 binary with $m_1 = 23.2M_\odot$ and

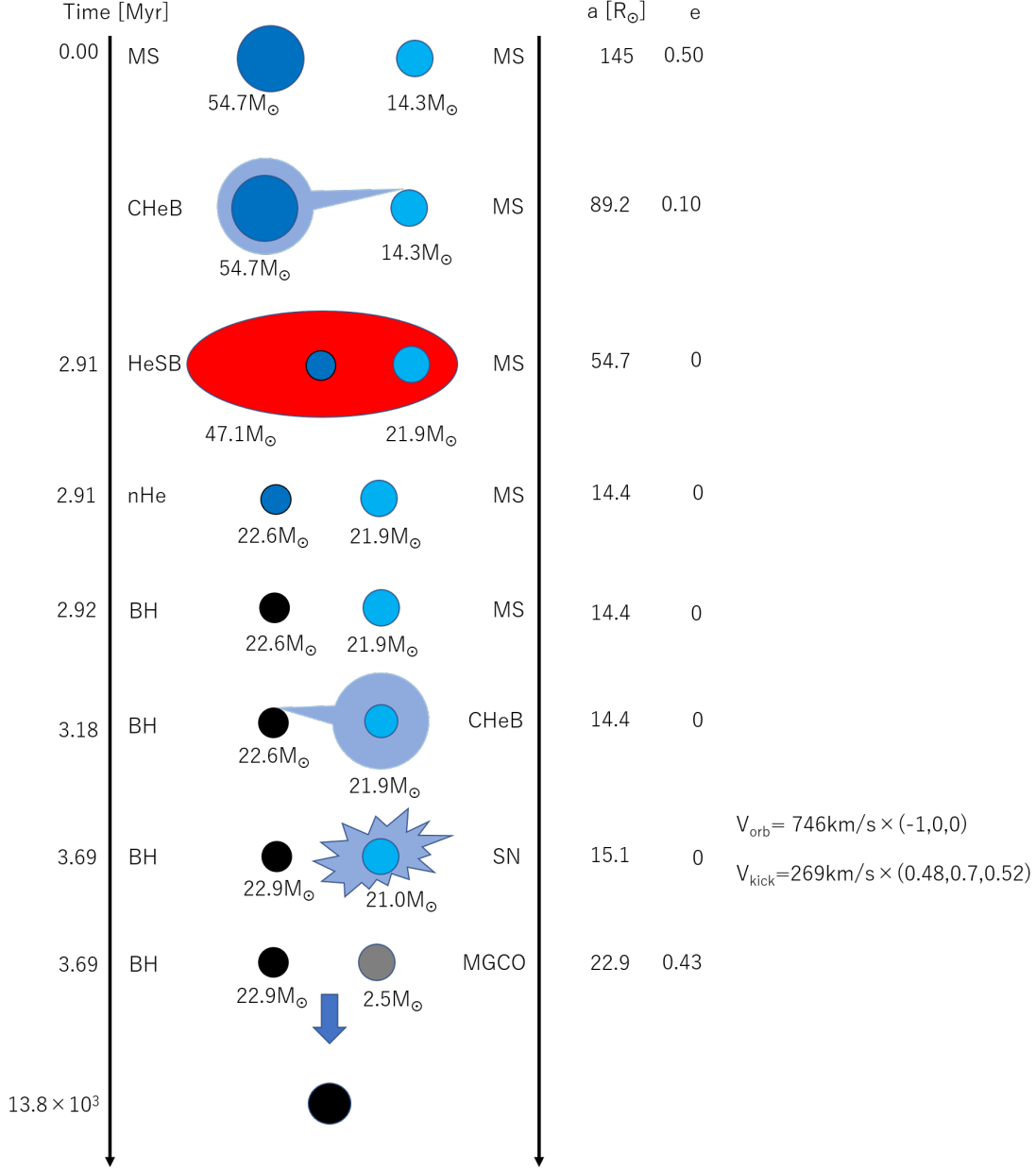


Fig. 3 Evolutionary path of a Pop III BH-MGCO binary similar to GW190814. MS, CHeB, HeSB, and nHe mean the main sequence, Core He burning, He shell burning, and naked He stars, respectively. The naked He star is the remnant after the common envelope phase. V_{orb} and V_{kick} are the orbital velocity just before the SN, and the natal kick velocity, respectively. a (in the solar radius R_{\odot}) and e denote the orbital separation and eccentricity, respectively.

$m_2 = 2.59 M_{\odot}$ becomes $z_{\text{max}} = 0.0814$ for LIGO O3a-Livingston, 0.211 for LIGO O5, 5.81 for ET-B, and 49.4 for CE2.

Table 1 shows the averaged masses of BH-MGCO binaries in the solar mass M_{\odot} for each kick model, and the event rates in $[\text{yr}^{-1}]$ based on the maximum observable redshifts z_{max} (shown as values in parenthesis for each detector) of this typical binaries for 4 GW detector

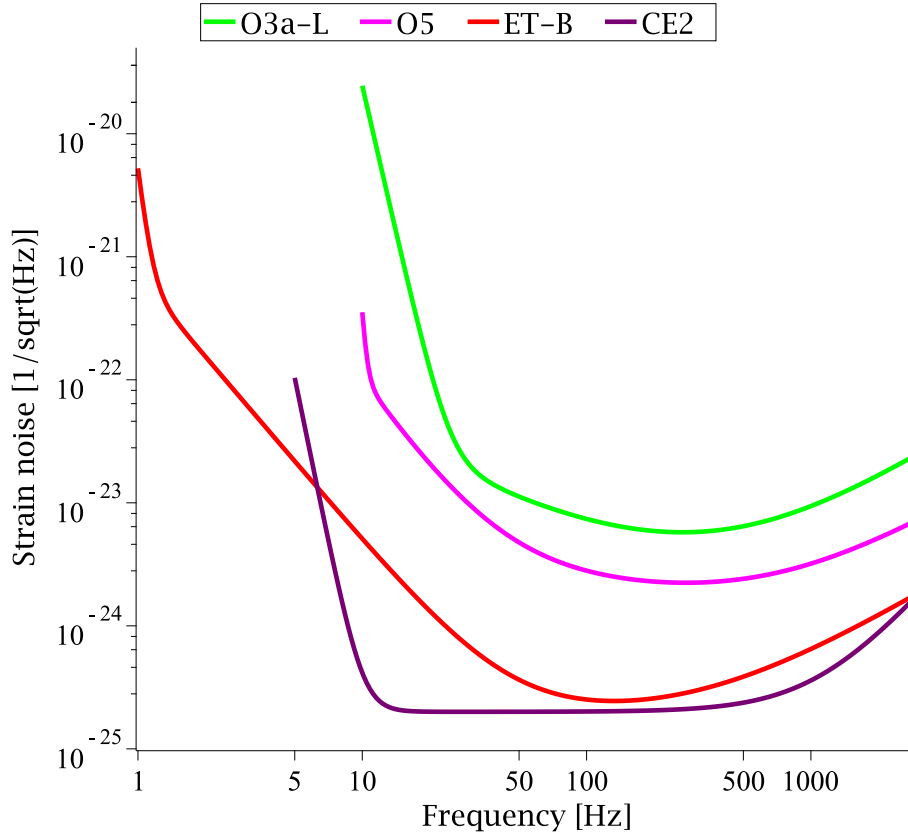


Fig. 4 Strain-noise fitted curves for 4 GW detector configurations: LIGO O3a-Livingston (O3a-L, green), LIGO O5 (O5, magenta), Einstein Telescope (ET-B) (red) and Cosmic Explorer (CE2) (purple). These fitting curves are obtained by using Refs. [32–35]. We have lower frequency cutoffs of 10 Hz, 1 Hz and 5 Hz for O3a-L and O5, ET-B and CE2, respectively.

configurations. For the O3a-L detector, the maximum event rate of GWs is 0.268 yr^{-1} for the kick model of $\sigma_k = 150 \text{ km/s}$. For the O5, ET-B and CE2 detectors, the maximum event rate of GWs are found as 3.62 yr^{-1} for the $\sigma_k = 100 \text{ km/s}$, 2070 yr^{-1} for the $\sigma_k = 265 \text{ km/s}$ and 3830 yr^{-1} for the $\sigma_k = 300 \text{ km/s}$, respectively.

3. *Discussion* In a binary system, a heavier BH is formed first. After that, a lighter NS is formed. At this time, a part of the blown outer layer with a mass of $\sim 1 M_\odot$ falls back, and the NS becomes a BH with a mass of $\sim 2.6 M_\odot$. Normally, this binary BH takes much longer time to coalesce than the Hubble time, but considering the kick velocity of the MGCO, the binary coalescence will occur within the Hubble time. Figure 5 shows mass distributions of MGCOs which merge within the Hubble time for each kick velocity model. As a future prediction, the lighter BHs can have various masses, and some may be NS. What seemed strange in the LIGO-Virgo paper [1] is commonplace in this scenario. The mass distribution of MGCOs (Fig. 5) does not depend on the kick velocity models, but depends on the SN remnant model. Our understanding of the central engine of supernova explosions and also the study of the explosions in Pop III are not yet complete. Future detections of MGCOs

Table 1 Averaged masses ($\langle m_1 \rangle, \langle m_2 \rangle$) of BH-MGCO binaries in the solar mass M_\odot and event rates in $[\text{yr}^{-1}]$ for 4 GW detector configurations: LIGO O3a-Livingston (O3a-L), LIGO O5 (O5), Einstein Telescope (ET-B) and Cosmic Explore (CE2) in 8 kick models with $\sigma_k = 0, 100, 150, 200, 265, 300, 400,$ and 500 km/s. Given the masses of binaries, we estimate the maximum observable redshift z_{max} (values in parenthesis for each detector), and then the event rates for each detector are derived by using the merger rate density calculated by the population synthesis simulations of Pop III stars. Although we can observe $z \sim 40$ by using the CE detector, the merger rate density is approximately 0 for $z \gtrsim 2.30$ in the cases of $\sigma_k = 0$, for $z \gtrsim 32.75$ in the cases of $\sigma_k = 100$ and 150 km/s, and for $z \gtrsim 33.30$ in the cases of $\sigma_k = 200, 265, 300, 400$ and 500 km/s.

σ_k (km/s)	$(\langle m_1 \rangle, \langle m_2 \rangle)$	O3a-L	O5	ET-B	CE2
0	(36.9, 2.91)	0.306 (0.106)	4.03 (0.277)	102 (6.39)	102 (35.2)
100	(32.1, 2.73)	0.207 (0.0960)	3.62 (0.250)	687 (6.13)	774 (38.7)
150	(31.2, 2.67)	0.268 (0.0938)	3.47 (0.244)	1440 (6.06)	1850 (39.4)
200	(30.9, 2.63)	0.225 (0.0927)	2.99 (0.241)	2020 (6.01)	3000 (39.6)
265	(30.5, 2.59)	0.194 (0.0914)	2.92 (0.238)	2070 (5.95)	3750 (39.9)
300	(30.3, 2.59)	0.158 (0.0912)	1.99 (0.237)	1940 (5.95)	3830 (40.1)
400	(30.3, 2.59)	0.111 (0.0912)	1.13 (0.237)	1560 (5.95)	3430 (40.1)
500	(30.4, 2.59)	0.0928 (0.0913)	1.24 (0.238)	1200 (5.95)	2700 (40.0)

may give a strong constraint on the SN remnant model. As a summary, the lighter compact objects will always become BH or NS which is close to the maximum mass of NS in the scenario of this letter.

In our simulation, the orbit of the binary before the supernova (SN) explosion of the secondary star after the BH formation of the primary star is eccentric in general. However in the eccentric orbit of the binary, it is very difficult to find the physical explanation of the effect of the kick velocity at the SN explosion using the analytic study so that we treat only a circular orbit before the SN explosion of the secondary star. We believe the essence of the physics can be obtained in our model.

Let us consider a binary with mass m_1 and m_2 ($< m_1$) in a circular orbit with the separation a . We define the total mass by $m_t = m_1 + m_2$. We take the center of the inertia at the origin of the x - y coordinates so that the location of the star 1 and the star 2 are at $\mathbf{r}_1 = (-a_1, 0)$ and $\mathbf{r}_2 = (a_2, 0)$ where $a_1 = (m_2/m_t)a$ and $a_2 = (m_1/m_t)a$, respectively. From the results of Newtonian dynamics, the total Energy E_0 , the angular momentum J_0 and the angular frequency Ω of the binary are given by

$$E_0 = -\frac{G m_1 m_2}{2a}, \quad J_0^2 = G m_1 m_2 \mu a, \quad \Omega = \sqrt{\frac{G m_t}{a^3}}, \quad (1)$$

and

$$\mu = \frac{m_1 m_2}{m_1 + m_2}, \quad (2)$$

where G is the gravitational constant. The y -direction rotational velocity v_1 and v_2 are given by

$$v_1 = -a_1 \Omega, \quad v_2 = a_2 \Omega. \quad (3)$$

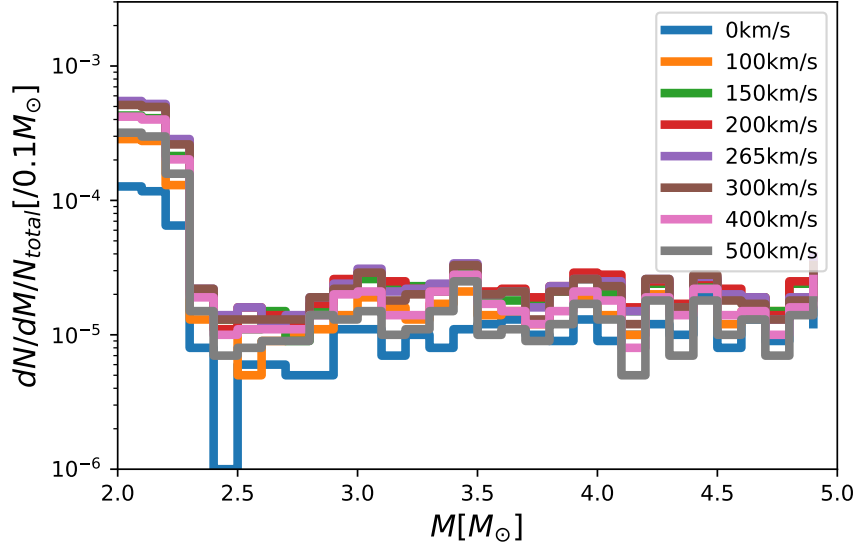


Fig. 5 Mass distributions of MGCOs which merge within the Hubble time for 8 kick models with $\sigma_k = 0, 100, 150, 200, 265, 300, 400,$ and 500 km/s. We find that the lighter BHs can have various masses.

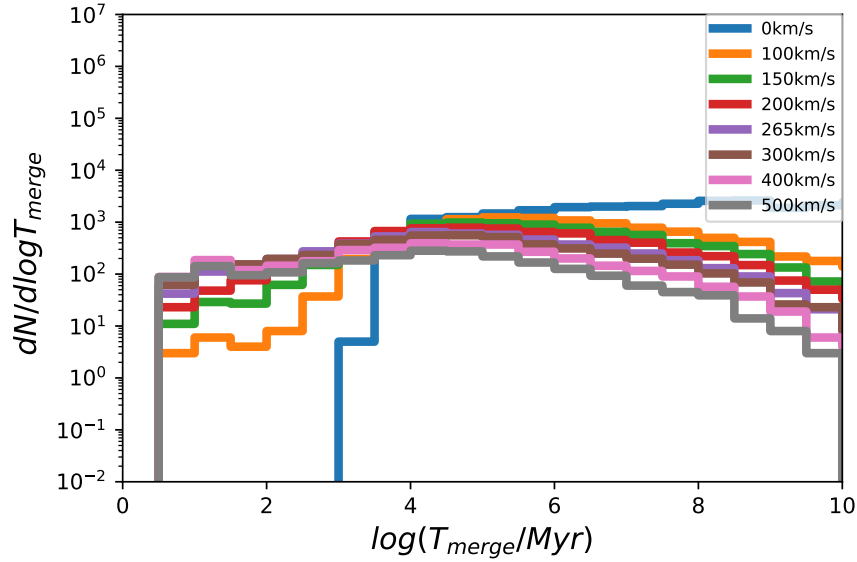


Fig. 6 Merger time distributions for 8 kick models with with $\sigma_k = 0, 100, 150, 200, 265, 300, 400,$ and 500 km/s.

Now we regard that the primary star is a BH with mass $m_1 = 23M_\odot$ and the secondary one with mass $m_2 = 21M_\odot$ explodes as a supernova explosion remaining mass gap compact object with mass $m'_2 = 2.5M_\odot$ and a kick velocity v_k along the y -direction for simplicity.

Before the supernova, we assume that the orbit of the binary is expressed by Eqs. (1) and (2) with the location of the BH at \mathbf{r}_1 and the pre-supernova secondary star at \mathbf{r}_2 . We treat the supernova as the instantaneous event so that after the supernova we regard that the secondary star turns out to be a mass gap compact object with mass m'_2 and only the y -direction velocity of $v'_2 = v_2 + v_k$ at \mathbf{r}_2 . The mass, location and velocity of the primary are not changed, that is, m_1 , \mathbf{r}_1 and $v'_1 = v_1$.

The new position vector \mathbf{r}_G of the center of mass becomes $\mathbf{r}_G = (\mathbf{r}_1 m_1 + \mathbf{r}_2 m'_2)/(m_1 + m'_2)$ so that the y -component velocity of each star in the center of mass coordinate are

$$v''_1 = \frac{m'_2(v_1 - v'_2)}{m_1 + m'_2}, \quad v''_2 = \frac{-m_1(v_1 - v'_2)}{m_1 + m'_2}. \quad (4)$$

To obtain the semi-major axis a_k and the eccentricity e_k after the supernova explosion with the kick velocity v_k , let us calculate the energy E_k and the angular momentum J_k in the center of mass coordinate as

$$E_k = \frac{1}{2}m_1(v''_1)^2 + \frac{1}{2}m'_2(v''_2)^2 - \frac{Gm_1m'_2}{a}, \quad (5)$$

$$J_k = (-a_1 - x_G)m_1v''_1 + (a_2 - x_G)m'_2v''_2, \quad (6)$$

where

$$x_G = \frac{-a_1m_1 + a_2m'_2}{m_1 + m'_2}. \quad (7)$$

Inserting Eq. (4) into Eqs. (5) and (6), we have

$$E_k = \frac{1}{2}\mu' \left\{ (a\Omega + v_k)^2 - \frac{2G(m_1 + m'_2)}{a} \right\}, \quad (8)$$

$$J_k = \mu'(a\Omega + v_k)a, \quad (9)$$

where

$$\mu' = \frac{m_1m'_2}{m_1 + m'_2}. \quad (10)$$

Using E_k and J_k , the new semi-major axis a_k and eccentricity e_k are given by

$$a_k = -\frac{Gm_1m'_2}{2E_k}, \quad 1 - e_k^2 = -\frac{2E_kJ_k^2}{G^2m_1^2m'_2{}^2\mu'}. \quad (11)$$

Now the merging time t_m due to the emission of the GWs is written as

$$t_m = \frac{5}{256} \frac{a_k^4}{c} \left(\frac{Gm_1}{c^2} \right)^{-1} \left(\frac{Gm'_2}{c^2} \right)^{-1} \left(\frac{G(m_1 + m'_2)}{c^2} \right)^{-1} (1 - e_k^2)^{3.5}. \quad (12)$$

Using Eqs. (8) and (9), Eq. (12) is written as

$$t_m = \frac{5}{256} \frac{1}{c} \left(\frac{Gm_1}{c^2} \right)^{-1} \left(\frac{Gm'_2}{c^2} \right)^{-1} \left(\frac{G(m_1 + m'_2)}{c^2} \right)^{-1} \frac{J_k^7}{\sqrt{-2E_k}G^3m_1^3m'_2{}^2\mu'^{\frac{7}{2}}}. \quad (13)$$

Figure 6 shows that if the kick velocity is zero, there are almost no mergers with a merging time less than $\sim 10^9$ yr. This means that no GW signal is observed from the merger of binary BH-mass gap compact object around $z \sim 10$ since the age of the universe at $z \sim 10$ is $\sim 4.5 \times 10^8$ yr which is much smaller than the merging time of the binary. One of the methods to have such mergers at $z \sim 10$ is to introduce the kick velocity in the SN explosion event of

the secondary. If $(a\Omega + v_k)$ decreases, J_k decreases and $\sqrt{-2E_K}$ increases from Eqs. (8) and (9) so that the merging time decreases from Eq. (13). Note here that to decrease $(a\Omega + v_k)$ under the same a , m_1 , m_2 and m' , v_k should be negative, that is, the direction of the kick is opposite to that of the rotation. The event rate of such mergers is roughly in proportion to the star formation rate such as de Souza et al. (2011) star formation model of Pop III stars (see Fig. 8 of Kinugawa et al. (2014)) adopted in our population synthesis simulation so that the formation of the binary starts from $z \sim 30$, has a peak at $z \sim 10$ and ends at $z \sim 5$. The merging time due to the emissions of GWs can be much smaller than the age of the universe for a given redshift z so that for a given kick velocity, the event rate as a function of the redshift is found to be similar to the star formation history in our population synthesis simulations. This theoretically expected behaviour of the merger rate as a function of z agrees with Fig. 2

For a fixed redshift z , our numerical simulation shows that the merging rate as a function of the kick velocity first increases, has a peak for $v_k \sim 300$ km/s and decreases again for $v_k > 300$ km/s. Since the merger rate for $v_k = 0$ is almost zero, it is natural that the merging rate first increases as a function of v_k . While in the extreme limit of the large kick velocity, almost all BH-mass gap compact object systems disrupt so that the above increase of the merging rate should be stopped at some value of v_k , and after that it should decrease as a function of v_k . In our case, we obtain the peak is $v_k \sim 300$ km/s from numerical simulation. Although it is difficult to get the peak value of the velocity dispersion σ_k analytically even in our circular orbit treatment of the binaries before SNe, we can confirm from the above physical arguments, the existence of the peak of the merger rate as a function of v_k for a given redshift z . To obtain the numerical value of v_k , the population synthesis calculations are indispensable since the analytic arguments are restricted to the initial circular orbit and the direction of the kick velocity parallel to the orbital velocity.

Using Eqs. (8)–(11), we can rewrite Eq. (12) as

$$\frac{a^4 \left(1 + \frac{v_k}{a\Omega}\right)^7}{\sqrt{2 \left(\frac{m_1+m_2'}{m_1+m_2}\right) - \left(1 + \frac{v_k}{a\Omega}\right)^2}} = \frac{256}{5} \left(\frac{Gm_1}{c^2}\right) \left(\frac{Gm_2'}{c^2}\right) \left(\frac{G(m_1+m_2')}{c^2}\right) \left(\frac{m_1+m_2'}{m_1+m_2}\right)^3 c t_m. \quad (14)$$

Inserting the adopted values of $m_1 = 23M_\odot$, $m_2 = 21M_\odot$ and $m_2' = 2.5M_\odot$, we have

$$\frac{a^4 \left(1 + \frac{v_k}{a\Omega}\right)^7}{\sqrt{1.159 - \left(1 + \frac{v_k}{a\Omega}\right)^2}} = (8.26 \times 10^{11} \text{ cm})^4 \left(\frac{t_m}{10^{10} \text{ yr}}\right). \quad (15)$$

As for the merger rate at $z = 0$, the merger time of the binary should be $t_m \sim 10^{10}$ yr so that even in the case of the zero kick velocity, some binaries merge at $z = 0$. Now for $t_m = 10^{10}$ yr, we can rewrite Eq. (15) as

$$a \sim 6.57 \times 10^{11} \text{ cm} \frac{\left\{1 - \frac{2}{0.159} \left(\frac{v_k}{a\Omega}\right) - \frac{1}{0.159} \left(\frac{v_k}{a\Omega}\right)^2\right\}^{\frac{1}{8}}}{\left(1 + \frac{v_k}{a\Omega}\right)^{\frac{7}{4}}}. \quad (16)$$

For $v_k = 0$, $a \sim 6.57 \times 10^{11}$ cm. While for $v_k \neq 0$ the binary with a defined by Eq. (16) merges at $z = 0$. For a given Gaussian kick velocity distribution with a velocity dispersion of σ_k , and for various $v_k \neq 0$ with a determined by Eq. (16), the merger time can be $t_m = 10^{10}$ yr

so that the number of mergers should increase compared with that for $v_k = 0$. However in the limit of extreme large σ_k , the merger rate should decrease again since the most of v_k in an extremely large σ_k can not satisfy Eq. (16). Therefore, we can confirm that the event rate as a function of σ_k , first increases, has a peak, and then decreases from this physical argument. So far, we adopted only the circular orbit initially. In reality, the circular orbit approximation of binaries is not the case in general so that it is hard to estimate the peak value of σ_k and the merger rate analytically. However from the above physical arguments we can confirm the existence of the peak of the event rate as a function of σ_k definitely. To estimate them, we need the population synthesis numerical simulations as we did in our paper.

Acknowledgment T. K. acknowledges support from University of Tokyo Young Excellent researcher program. T. N. acknowledges support from JSPS KAKENHI Grant No. JP15H02087. H. N. acknowledges support from JSPS KAKENHI Grant Nos. JP16K05347 and JP17H06358.

References

- [1] R. Abbott *et al.* [LIGO Scientific and Virgo], *Astrophys. J.* **896**, L44 (2020) [arXiv:2006.12611 [astro-ph.HE]].
- [2] <https://emfollow.docs.ligo.org/userguide/glossary.html>
- [3] S. Rastello, M. Mapelli, U. N. Di Carlo, N. Giacobbo, F. Santoliquido, M. Spera, A. Ballone and G. Iorio, [arXiv:2003.02277 [astro-ph.HE]].
- [4] T. Broadhurst, J. M. Diego and G. F. Smoot, [arXiv:2006.13219 [astro-ph.CO]].
- [5] M. Zevin, M. Spera, C. P. L. Berry and V. Kalogera, [arXiv:2006.14573 [astro-ph.HE]].
- [6] E. R. Most, L. J. Papenfort, L. R. Weih and L. Rezzolla, [arXiv:2006.14601 [astro-ph.HE]].
- [7] K. Vattis, I. S. Goldstein and S. M. Koushiappas, [arXiv:2006.15675 [astro-ph.HE]].
- [8] H. Tan, J. Noronha-Hostler and N. Yunes, [arXiv:2006.16296 [astro-ph.HE]].
- [9] M. Safarzadeh and A. Loeb, [arXiv:2007.00847 [astro-ph.HE]].
- [10] R. Essick and P. Landry, [arXiv:2007.01372 [astro-ph.HE]].
- [11] N. B. Zhang and B. A. Li, [arXiv:2007.02513 [astro-ph.HE]].
- [12] K. Jedamzik, [arXiv:2007.03565 [astro-ph.CO]].
- [13] Y. D. Tsai, A. Palmese, S. Profumo and T. Jeltema, [arXiv:2007.03686 [astro-ph.HE]].
- [14] F. J. Fattoyev, C. J. Horowitz, J. Piekarewicz and B. Reed, [arXiv:2007.03799 [nucl-th]].
- [15] I. Mandel, B. Mueller, J. Riley, S. E. de Mink, A. Vigna-Gomez and D. Chattopadhyay, [arXiv:2007.03890 [astro-ph.HE]].
- [16] Y. Yang, V. Gayathri, I. Bartos, Z. Haiman, M. Safarzadeh and H. Tagawa, [arXiv:2007.04781 [astro-ph.HE]].
- [17] A. Tsokaros, M. Ruiz and S. L. Shapiro, [arXiv:2007.05526 [astro-ph.HE]].
- [18] I. Tews, P. T. H. Pang, T. Dietrich, M. W. Coughlin, S. Antier, M. Bulla, J. Heinzel and L. Issa, [arXiv:2007.06057 [astro-ph.HE]].
- [19] S. Clesse and J. Garcia-Bellido, [arXiv:2007.06481 [astro-ph.CO]].
- [20] Y. Lim, A. Bhattacharya, J. W. Holt and D. Pati, [arXiv:2007.06526 [nucl-th]].
- [21] V. Dexheimer, R. O. Gomes, T. Klöhn, S. Han and M. Salinas, [arXiv:2007.08493 [astro-ph.HE]].
- [22] A. Sedrakian, F. Weber and J. J. LI, [arXiv:2007.09683 [astro-ph.HE]].
- [23] Z. Roupas, [arXiv:2007.10679 [gr-qc]].
- [24] D. A. Godzieba, D. Radice and S. Bernuzzi, [arXiv:2007.10999 [astro-ph.HE]].
- [25] T. Kinugawa, T. Nakamura and H. Nakano, *PTEP* **2017**, 021E01 (2017) [arXiv:1610.00305 [astro-ph.HE]].
- [26] T. Kinugawa, K. Inayoshi, K. Hotokezaka, D. Nakauchi and T. Nakamura, *Mon. Not. Roy. Astron. Soc.* **442**, 2963-2992 (2014) [arXiv:1402.6672 [astro-ph.HE]].
- [27] K. Belczynski, V. Kalogera and T. Bulik, *Astrophys. J.* **572**, 407-431 (2001) [arXiv:astro-ph/0111452 [astro-ph]].
- [28] C. S. Kochanek *Mon. Not. Roy. Astron. Soc.* **493** 4945 (2020) [arXiv:2001.07216 [astro-ph.SR]].
- [29] T. Nakamura, M. Ando, T. Kinugawa, H. Nakano, K. Eda, S. Sato, M. Musha, T. Akutsu, T. Tanaka, N. Seto, N. Kanda and Y. Itoh, *PTEP* **2016**, 093E01 (2016) [arXiv:1607.00897 [astro-ph.HE]].

-
- [30] P. Ajith, M. Hannam, S. Husa, Y. Chen, B. Bruegmann, N. Dorband, D. Muller, F. Ohme, D. Pollney, C. Reisswig, L. Santamaria and J. Seiler, *Phys. Rev. Lett.* **106**, 241101 (2011) [arXiv:0909.2867 [gr-qc]].
- [31] N. Dalal, D. E. Holz, S. A. Hughes and B. Jain, *Phys. Rev. D* **74**, 063006 (2006) [arXiv:astro-ph/0601275 [astro-ph]].
- [32] B. P. Abbott *et al.* [KAGRA, LIGO Scientific and VIRGO], *Living Rev. Rel.* **21**, 3 (2018) [arXiv:1304.0670 [gr-qc]].
- [33] S. Hild, S. Chelkowski and A. Freise, [arXiv:0810.0604 [gr-qc]].
- [34] C. K. Mishra, K. G. Arun, B. R. Iyer and B. S. Sathyaprakash, *Phys. Rev. D* **82**, 064010 (2010) [arXiv:1005.0304 [gr-qc]].
- [35] D. Reitze, R. X. Adhikari, S. Ballmer, B. Barish, L. Barsotti, G. Billingsley, D. A. Brown, Y. Chen, D. Coyne, R. Eisenstein, M. Evans, P. Fritschel, E. D. Hall, A. Lazzarini, G. Lovelace, J. Read, B. S. Sathyaprakash, D. Shoemaker, J. Smith, C. Torrie, S. Vitale, R. Weiss, C. Wipf and M. Zucker, *Bull. Am. Astron. Soc.* **51**, 035 [arXiv:1907.04833 [astro-ph.IM]].